Mechanical Technology and Engineering Insights

www.mtei.reapress.com

Research Expansion Alliance

Mech. Technol. Eng. Insights. Vol. 3, No. 1 (2026) 69–80.

Paper Type: Original Article

# Concurrent Detection of Surface and Subsurface Defects via Phased Array Ultrasonic Multiple Inspection: A Finite Element Simulation Study

**Omar Mar Cornelio[1,*], Mansour Nikkhah Bahrami[2]**

[1] Center for Computational Mathematics Studies, University of Computer Sciences, 19370 La Habana, Cuba; omarmar@uci.cu.

[2] Department of Mechanical Engineering, College of Engineering, University of Tehran, Iran; mbahrami@ut.ac.ir.

**Citation:**

| | |
|---|---|
| *Received: 06 April 2025*<br>*Revised: 21 July 2025*<br>*Accepted: 11 September 2025* | Cornelio, O. M. & Nikkhah Bahrami, M. (2026). Concurrent detection of surface and subsurface defects via phased array ultrasonic multiple inspection: A finite element simulation study. *Mechanical Technology and Engineering Insights*, *3*(1), 69-80. |

## Abstract

The question of decreasing the time of inspections while increasing their detection accuracy still appears crucial in modern industrial settings. The use of advanced techniques of Nondestructive Testing (NDT) has made it possible to increase performance and improve the accuracy of the inspection process. Ultrasonic phased array techniques proved to be a breakthrough technology that allows conducting more accurate performance assessments of components of industrial equipment with increased efficiency. In this research paper, a numerical analysis of the newly developed inspection technique based on the unique properties of the ultrasonic phased array technique will be presented. It aims at combining the ability to steer and focus beams of a phased array transducer with the high surface sensitivity of Rayleigh waves to develop a multiple inspection technique. The developed method provides the possibility to detect surface defects and volumetric defects during a single inspection procedure. The results of simulations show that Rayleigh waves possess high stability of the amplitude with regard to the propagation distance and angle of steering; therefore, they are very suitable for surface defect detection. At the same time, the Time-of-Flight Diffraction (ToFD) technique used with a single probe configuration allows detecting embedded cracks with sufficient accuracy.

**Keywords:** Nondestructive testing, Ultrasonic phased array, Time-of-flight diffraction, Surface defect detection.

## 1 | Introduction

The development of ultrasonic signals that can at the same time detect both planar and surface defects is indeed an innovative idea in the field of Nondestructive Testing (NDT). Several studies in recent times have been performed on this topic, but using different methodologies to achieve this goal [1], [2]. In the current work, we introduce for the first time a multiple inspection simulation method which is able to detect both surface defects and internal cracks.

Corresponding Author: omarmar@uci.cu

https://doi.org/10.48313/mtei.v3i1.81

Simulation forms the first phase in Ultrasonic Testing (UT) modelling and helps in gaining insight into the testing process. Predictive models aid in determining the best parameter settings and create mathematical models of the physical system that react consistently to changes in input parameters. FE ultrasonic modelling was first introduced by Ludwig and Lord [3] and paved the way for further developments in this area. Simulation in phased array testing has proved especially useful in determining the favourable transducer properties and parameters.

There has been considerable interest in the Time-of-Flight Diffraction (ToFD) method due to its capability of precise characterization of flaws on planar surfaces. The accuracy of depth and length measurements in this method is much greater than that in conventional methods based on amplitude measurements. The finite element modeling of ToFD has been considered by Baskaran et al. [4] and Honarvar and Khorasani [5]. The recent developments in this field have allowed the usage of the ToFD technique for austenitic welds [6], as well as the analysis of ToFD for unequal thickness specimens [7], and the development of new curved-sole probes for improved inspection.

When it comes to surface crack testing, the best ultrasonic method is the application of Rayleigh waves. Silk [8] formulated the basics of using ultrasonic surface waves for determination of crack penetrations. These waves propagate close to the free surface of the material and have exponential decay with depth. The energy concentration in the thin surface layer makes them very sensitive to surface defects. Moreover, these waves can trace complicated curvatures, making it possible to examine hard-to-reach defects.

Date et al. [9] demonstrated the high accuracy of ultrasonic timing methods using Rayleigh waves for characterizing slots as shallow as 0.8 mm. Hévin et al. [10] determined surface crack depths in concrete with 15% accuracy using spectral analysis, while Scala and Bowles [11] achieved better than 50 µm accuracy for 0.5 mm deep slots using transmitted near-field measurements.

Date et al. [9] proved high precision of ultrasonic timing procedures with Rayleigh waves for detecting slots up to 0.8 mm depth. The surface crack depths in concrete were evaluated with 15% accuracy by Hévin et al. [10] with a spectral analysis procedure, whereas Scala and Bowles [11] provided detection precision better than 50 µm for slots of 0.5 mm depth with a transmitted near-field technique.

The recent research has greatly enhanced the applications of Rayleigh waves in NDT. Verma and Bélanger [12] have introduced a new pulse echo Rayleigh wave procedure for surface crack measurement with no usage of wedges and with sizing accuracy better than 5% error by means of signal averaging techniques. In addition to this, this technique solves the problem of loss of signal energy due to couplant, which had been limiting the Rayleigh wave applications for a long time. Liu et al. [13] have introduced an imaging technique based on leaky Rayleigh waves using an ultrasonic phased array with Total Focusing Method (TFM). Furthermore, the excitation of Rayleigh waves with phased array transducers and linear time delay law is now possible [14].

Application of such waves to characterizing surface-breaking cracks in tubular structures [15] and study of the interaction between the wave and rolling contact fatigue defect by numerical simulation [16] were also explored.

The use of finite element modeling in the simulation of ultrasonic phased arrays continues to be an active area of research. Kolkoori et al. [17] proposed a three-dimensional hybrid modeling technique that combines finite element analysis with semianalytical simulation in order to model the propagation of waves in heavy plates for porosity testing and showed good quantitative agreement with experimental results. Also, a recent review of sound field modeling techniques and imaging technology for ultrasonic phased arrays is presented [18]. Innovative techniques include multimodal image fusion [19], machine learning-enhanced characterization of surface defects based on Rayleigh wave [20], and principal component analysis for TFM imaging with Rayleigh wave [21]. In addition, novel techniques include laser-generated Rayleigh waves in coating/substrate structure [22] and guided wave phased array ultrasonic imaging for thin plate [23].

This research paper is an attempt to further consolidate these ideas through a multiple inspection technique which makes use of phased array beam steering along with the ToFD concept and Rayleigh waves to detect and characterize surface as well as subsurface defects.

# 2|FEM Modelling of TOFD Method

The commercial FEM package ABAQUS6.11 is used for two-dimensional modelling of ultrasonic wave propagation. The physical properties of the block are as follows: E = 60 GPa, ϱ= 2240 kg/m3, and υ= 0.244. The entire area of the sample is discretised into standard two-dimensional spatial Square Plane Strain Elements (CPE4R) with linear shape functions and four nodes, where each node has two degrees of freedom with respect to displacement. In order to get more accurate results, we can decrease element size, but there are limitations. These limitations occurred due to limited computer system capacity to calculate the enormous calculations needed for simulation. According to the previous work [24], mesh size ($\Delta d$) should satisfy *Eq. (1)*:

$$\Delta d \leq \lambda/15, \tag{1}$$

where $\lambda_{min}$ is the shortest wavelength at the excitation frequency of the simulated waves, and Δd is the dimension of the element. Our trial and error studies showed that in order to have a low computation time and good convergence, a mesh size in the order of 5 × 10^-5 m should be chosen.

## 2.1|Modeling of Transmitting Transducer

In this study, actual piezoelectric mechanisms have been modeled by the relevant transient pressure excitation. This excitation is a narrowband tone burst pulse of a certain frequency, which is applied on the 0.3mm distance on the top surface of the sample block. 32 elements were designed and excited. In other words, an ultrasonic pulse was introduced as a transient excitation pulse, which was applied as pressure on the width of each element. This pulse is given in *Eq. (2)*, where f is the excitation frequency, and N is the number of cycles of force.

$$F = \left[1 - \cos\left(\frac{2\pi f}{N}t\right)\right]\cos(2\pi f t), \qquad 0 < t < \frac{N}{f}. \tag{2}$$

In order to propagate an oblique ultrasonic wave by a phased array probe, we use a time delay law. These time delays, which are applied to adjacent phased array elements, are computed with Huygens' principle, as stated in *Eq. (3)*:

$$\Delta t = \frac{d \sin \theta_s}{C}, \tag{3}$$

where “d" is the distance between two adjacent elements, $\theta_s$ is the steering angle or propagation angle, "C" is the longitudinal wave velocity in the medium, and Δt is the time delay between two adjacent elements.

## 2.2|Modeling of Receiving Transducer

Since the basis of piezoelectric transducer operation is the conversion of electrical pulses to mechanical pressure and vice versa, we consider a "set point" on the surface as the receiver probe. Acceleration amplitude variations of this "set point" are regarded as amplitude variations in simulations in order to increase accuracy and quality of simulations.

# 3|Convergence Test

One of the most important parts of validation of the simulated model is the "convergence test" for FEM simulation. In order to discuss convergence results, different element sizes are considered. An amplitude diagram of the center node of the probe from the top crack tip is used to discuss the convergence results. Signal-to-noise ratio is obtained from received signals and plotted against element size in *Fig. 1*. For elements smaller than 50 μm, the SNR is stabilized and has a constant value approximately.

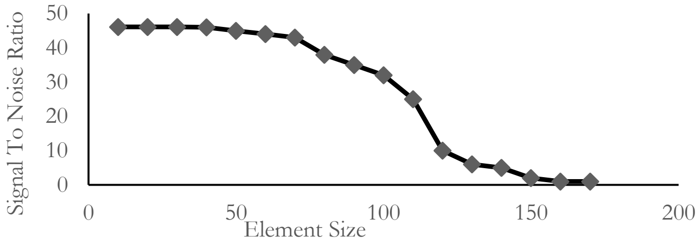


**Fig. 1. Signal-to-noise ratio obtained from received signals.**

## 3.1 | Interaction of Phased Array Ultrasonic Waves with Embedded Crack

After a phased array transducer is excited, longitudinal (I) and shear (II) waves are propagated in the bulk of the simulated steel block. Also, lateral longitudinal wave (III), lateral shear wave (IV), and Rayleigh wave (V) are transmitted along the surface. The head wave is denoted by (VI) (*Fig. 2*). After the Longitudinal wave incident on the crack, a sharp crack tip, like a source of waves, emits a wave. These diffracted waves from the crack tips are applied for the ToFD method; the first diffracted wave from the top crack tip, denoted by "VII," is the "Top Longitudinal Diffraction" wave, or "TLD". The second diffracted wave is the "Top shear diffraction" wave, or "TSD", indicated by "VIII", and the bottom diffraction waves are denoted by (IX) and (X), as shown in *Fig. 3* and *Fig. 4*.

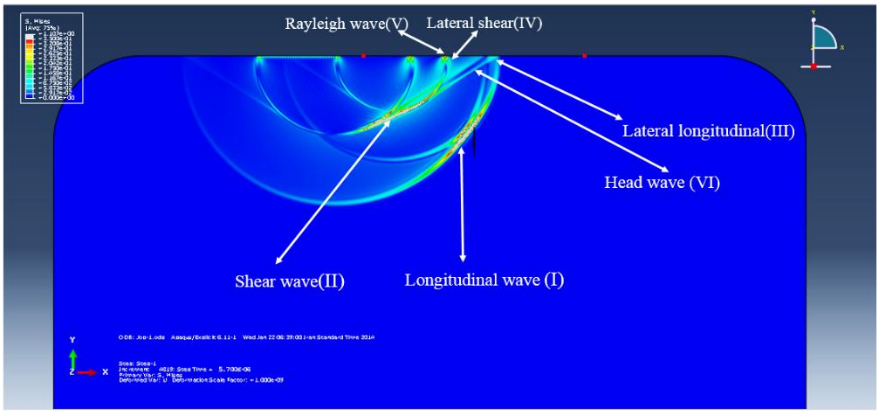


**Fig. 2. Snapshot of Abaqus viewport at 5.7(μs).**

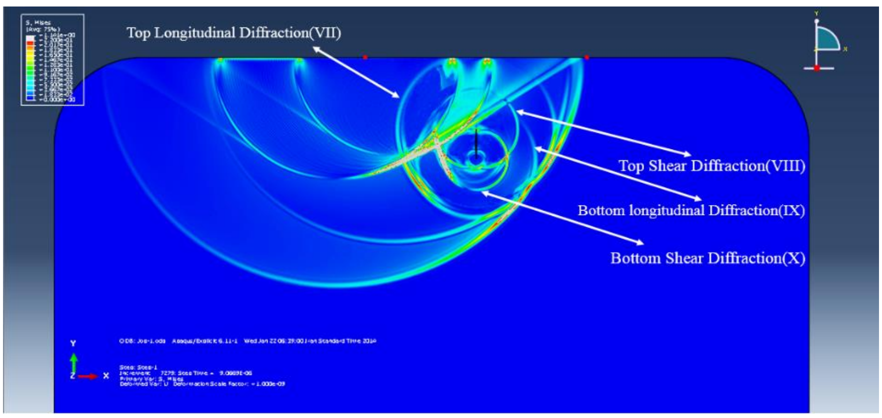


**Fig. 3. Snapshot of Abaqus viewport at 9.066(μs).**

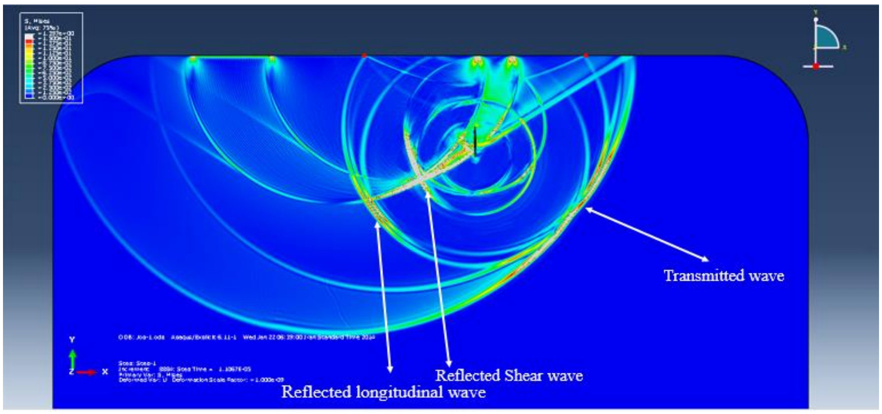


**Fig. 4. Snapshot of Abaqus viewport at 11.088(μs).**

## 3.2 | Effect of Wave Angle Variation on Amplitude of Waves

*Fig. 5* is the diagram of variation of "lateral longitudinal" wave amplitude by change in angle of wave. The slope of the curve is greater for angles that are wider than 60′; in other words, "Lateral longitudinal" wave amplitude increased more. For angles less than 40′, "lateral longitudinal" received amplitudes were reduced too much in comparison with angles greater than 60′.

*Fig. 5* indicates that "lateral longitudinal" amplitudes are related significantly to the angle of the wave. If it is used for surface defect detection, then the wave angle should be considered as a highly limiting parameter. "Lateral shear" wave amplitude variations plotted against wave angle variations. Measured amplitudes increase with increasing the angle of the oblique wave. *Fig. 7* denotes the high dependency of "lateral shear" wave on wave angles. For angles less than 45′ "lateral shear" wave measured amplitude has small amount and it is hard to distinguish it from noise.

*Fig. 8* indicates the variation of Rayleigh wave amplitudes by change in angle of wave. It is obvious from this figure that Rayleigh wave amplitudes are not affected by angle variation of the wave. According to *Figs. 5* and *6*, which show the effects of change in the wave angle parameter on received signals, it can be concluded that a single type of surface wave, which is not affected by angle variations, is the Rayleigh wave. Rayleigh wave is not considerably affected by angle variation, and it has a constant amplitude value even for oblique waves that are smaller than 40 degrees.

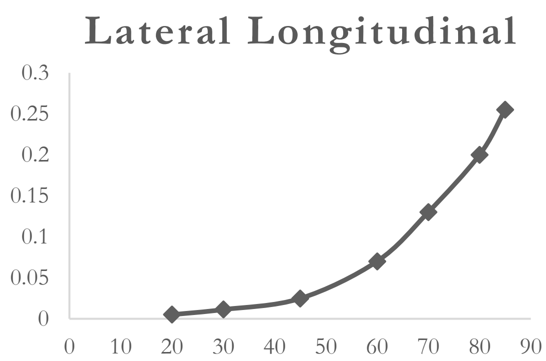


**Fig. 5. Effect of angle variation on amplitude of lateral longitudinal wave.**

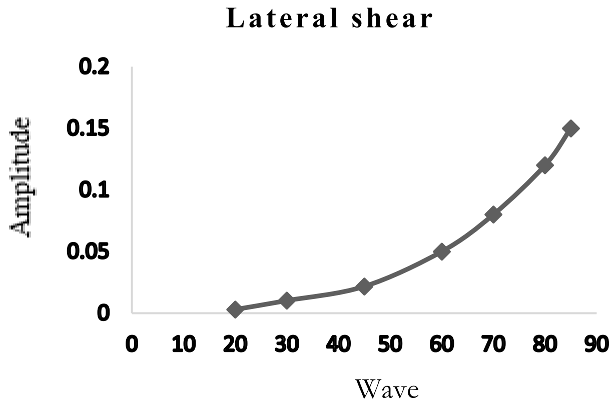


**Fig. 6. Effect of angle variation on amplitude of lateral shear wave.**

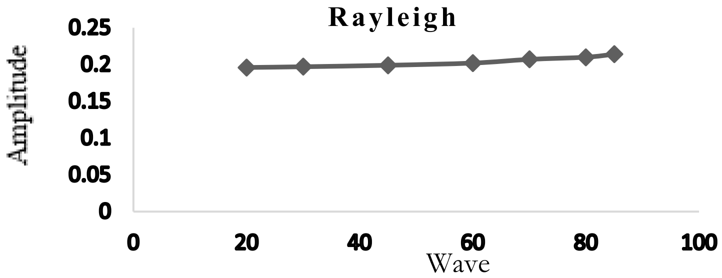


**Fig. 7. Effect of angle variation on amplitude of Rayleigh wave.**

## 3.3 | Effect of Distance on Amplitude of Surface Waves

As shown in *Fig. 8*, the lateral longitudinal wave amplitude decreases by increasing the distance of the receiving transducer from the transmitter. The received "Lateral longitudinal" echo for a transducer which is located at 1cm distance from the transmitting transducer has a maximum value due to the short distance between transmitter and receiver. In the first 4cm distance from the transmitter, "lateral longitudinal" wave amplitude decreases rapidly, but in the next 4cm distance, the slope of the curve is much less.

*Fig. 9* demonstrates that the lateral longitudinal wave has a high decreasing value, especially at near distances from the transmitting probe. When the "Lateral longitudinal" wave travels 8cm, its amplitude is reduced significantly. "Lateral shear" variations with distance are plotted in *Fig. 9*. After 4cm distance, the "Lateral shear" wave decreases significantly; between 2cm and 4 cm, the slope of the curve, i.e., the ratio of "Lateral shear" amplitude variations with respect to distance from the transmitter transducer, is greater than other parts of the curve; in other words, in this area, the "Lateral shear" wave amplitude reduced a lot. "Lateral shear" and "Lateral longitudinal" wave amplitudes decrease a lot after passing 6cm and 8 cm, respectively. It is a warning notation in surface defect detection. If defects are located outside this zone (6cm and 8cm from the transmitting transducer), using "Lateral longitudinal" and "Lateral shear" waves for defect detection does not yield recognizable results. *Fig. 10* shows the relation between Rayleigh wave amplitude and Rayleigh wave travelling distance. Rayleigh waves are not affected by distance variations. They have constant amplitudes even at far distances, where other types of surface waves disappear. In addition to the positive feature stated in the previous section, the constant amplitude of Rayleigh waves with distance variations is another main positive aspect of Rayleigh waves for surface defect detection.

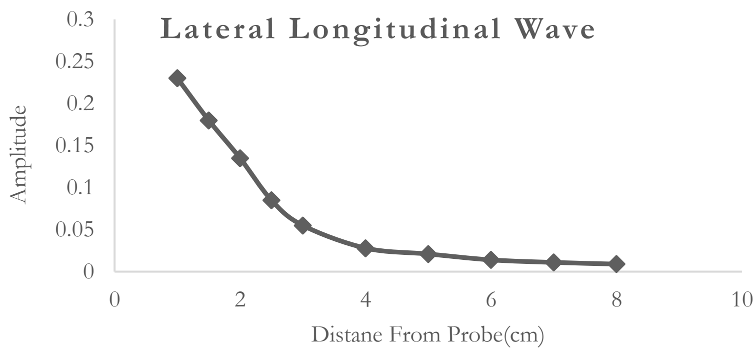


**Fig. 8. Effect of variation of distance on amplitude of lateral longitudinal waves.**

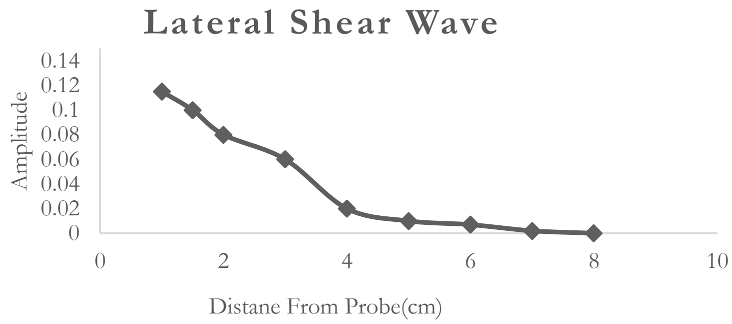


**Fig. 9. Effect of variation of distance on amplitude of lateral longitudinal waves.**

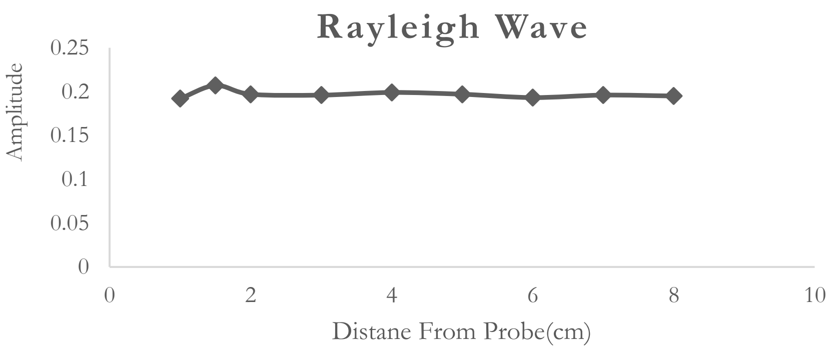


**Fig. 10. Effect of variation of distance on amplitude of lateral longitudinal waves.**

## 3.4 | Crack Sizing by ToFD with Single Probe Technique in Various Depths

*Fig. 11* shows his method schematically. Crack depth varies from 10mm to 75mm. Crack length is 7mm and is perpendicular to the scanning surface. Normal distance between the centerline of the probe and the crack body(S) is 2.5cm. cracks were located in 1,2,3,4,5,5.5,6,6.5,7,7.5 far from surface and normal distance between cracks and centerline of probe is 2.5cm. Diffracted waves from crack tips were detected well, and the A-scan was analyzed; the results are shown in *Fig. 13*. A-scan signal of a sample block with an embedded crack at a depth of 2 cm is shown in *Fig. 14*. All received echoes before 4 μs, which spread on the time axis, are initial pulses(V) and appear due to phased array excitation pulses at the center node of the probe. In *Fig. 12*, four main diffraction signals are observed in the received signal. In *Fig. 13*, the Top longitudinal diffraction (I) and the Bottom longitudinal diffraction (II) are received at 11.088 µs and 12.680 µs and define a crack size with 3.9% error. Shear diffraction signals are sensed after longitudinal diffraction waves.

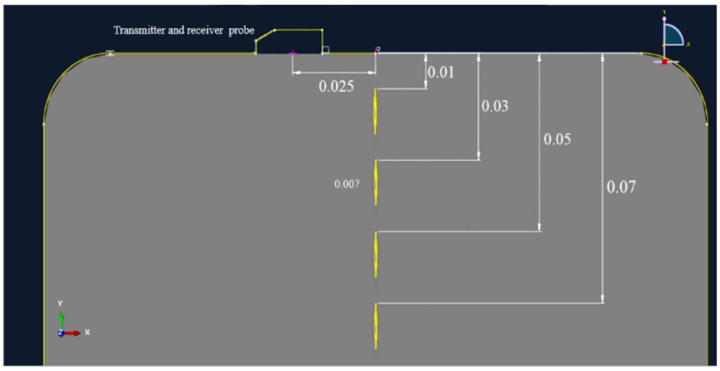


**Fig. 11. Crack sizing by TOFD with single probe technique in various depths.**

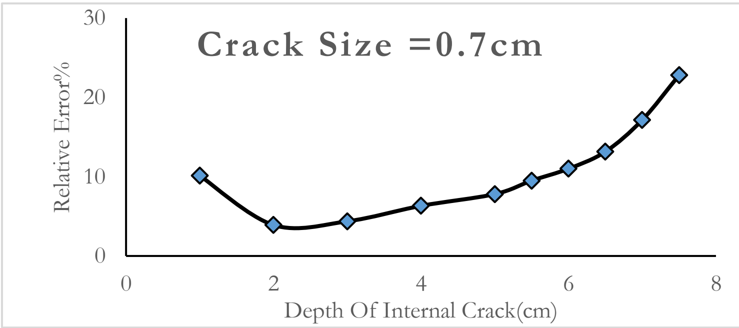


**Fig. 12. The variation of relative error for crack sizing by the TOFD method with a single probe in different depths.**

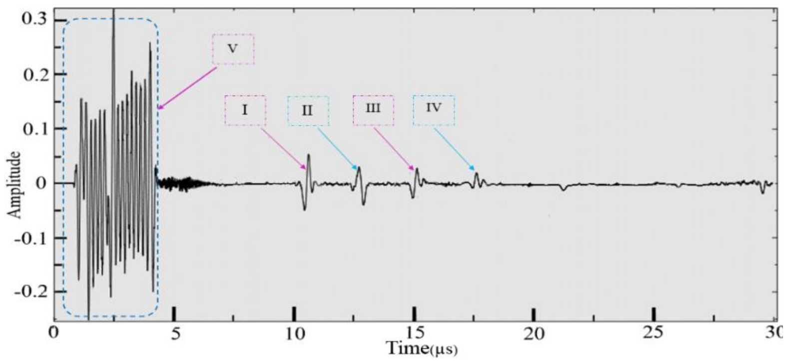


**Fig. 13. A-scan signal from a sample that has a crack at 2cm depth.**

## 3.5 | Multiple Detection of Surface and Planar Defect

The effect of angle variation and also increasing distance on surface waves has been discussed in the section on Rayleigh waves; from two main aspects, Rayleigh waves are in priority for surface defect detection. At first, the constant amplitude of the Rayleigh wave with increasing distance motivates us to apply this wave for defect detection; another aspect is amplitude stability by angle variations. ToFD with a single probe is simulated completely. In this section, a single probe is used as both the transmitter and receiver probe for nondestructive evaluation of crack and surface defect detection simultaneously for the first time. A-scan received signal clearly shows the crack diffraction echoes and also Rayleigh reflection waves. Finally, an A-scan that determines defects and also characterizes internal cracks is obtained. *Fig. 14a* shows an A-scan of a sample that has a crack of 1cm length in 2cm depth and also a surface defect 22.14 cm far from the center of the phased array transducer.

*Fig. 14b* and *14c* are magnified views of the first 40(µs) and last 40(µs); reflected and diffracted waves can be observed in *Fig. 14a*. Because of the long A-scan time, parts of it are enlarged. In the first 40 µs, an embedded crack is detected by the ToFD method, and evaluation of the diffraction received echoes indicates a crack of 9.5mm length, with a 4.2% error.

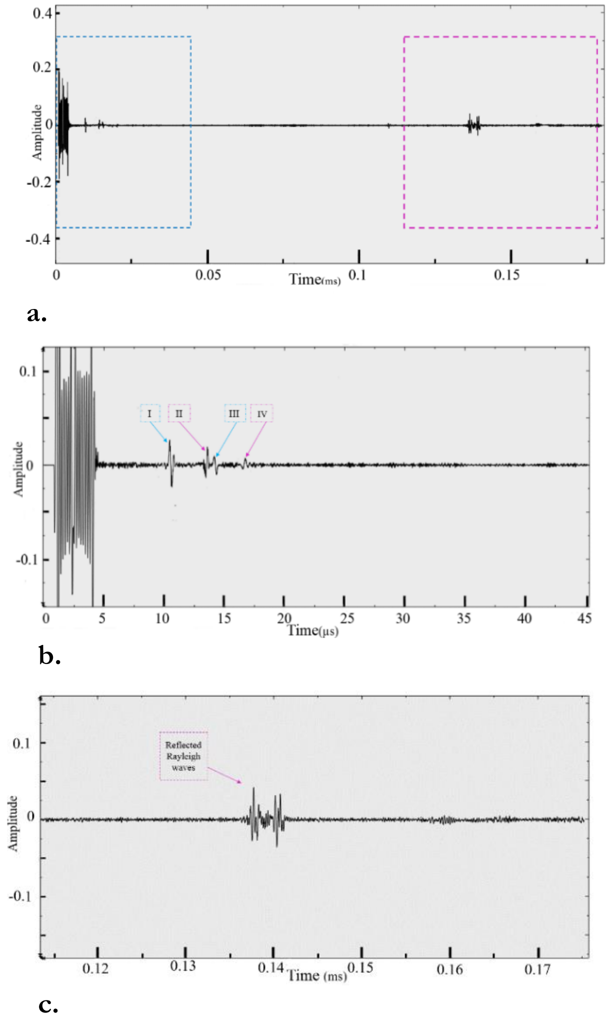


**Fig. 14a. Multiple A-scan signal which shows both internal crack and surface defect; b. magnified view of the first 40(µs) of Fig. 15a, which shows a 9.57 mm crack inside a block, c. magnified view of the last 40(µs) of Fig. 15a, which shows a surface defect at 19.967cm far from the probe.**

The accuracy of Rayleigh wave in surface defect detection is shown in *Fig. 15*. The error growth rate variation is negative and low, and also after the defect distance from the probe is increased to 18cm, it descends further.

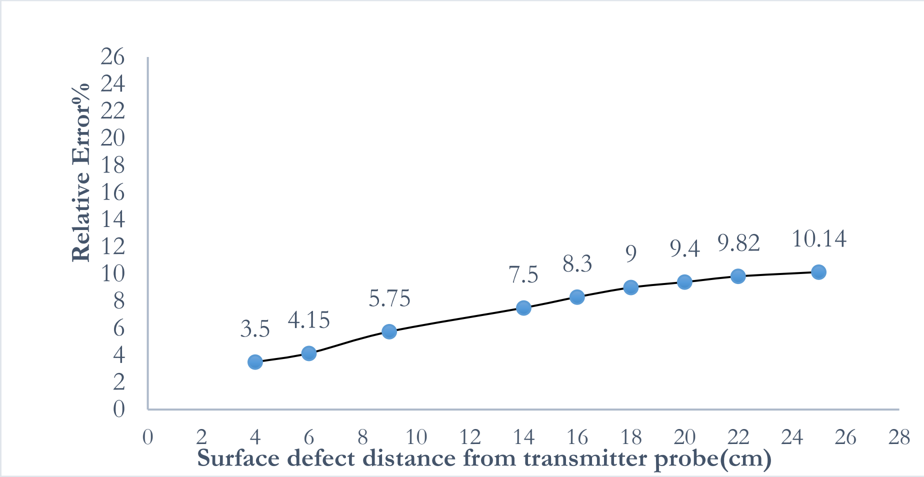


**Fig. 15. Accuracy of Rayleigh wave in surface defect detection by increasing defect distance.**

## 4 | Conclusion

This study presents a comprehensive finite element investigation of a novel multiple inspection methodology for simultaneous surface and subsurface defect detection using ultrasonic phased array technology. The following conclusions are drawn:

I. Rayleigh wave superiority for surface inspection: Among surface wave modes, Rayleigh waves exhibit unique advantages for surface defect detection. They maintain constant amplitude with propagation distance, preserving energy even at extended ranges where other surface waves attenuate completely. Additionally, Rayleigh waves are the only surface wave mode unaffected by steering angle variations, maintaining consistent amplitude regardless of beam angle.

II. ToFD single-probe crack characterization: Error analysis of single-probe ToFD for cracks of constant length at various depths reveals that accurate crack sizing is achieved for depths from 1 cm to 6 cm. The critical depth range for reliable crack size evaluation is 6 cm to 8 cm, beyond which accuracy diminishes.

III. Multiple defect detection validation: Simulation of the multiple detection method, a novel approach combining surface and subsurface defect evaluation, has been successfully demonstrated. This method leverages the high capabilities of ultrasonic phased array systems to achieve comprehensive defect characterization in a single inspection procedure.

IV. Surface defect detection accuracy: Rayleigh wave-based surface defect detection achieves less than 10% error at distances up to 24 cm from the transducer, confirming the effectiveness of this approach for practical industrial applications.

The proposed multiple inspection method represents a significant advancement in ultrasonic nondestructive evaluation, offering the potential for reduced inspection time, enhanced detection capabilities, and more comprehensive material assessment.

## Conflict of Interest

The authors declare that they have no competing interests.

## Data Availability

The data supporting the findings of this study are available within the article.

## Funding

This research did not receive any external funding.

# References

[1] Ernst, R., Weder, M., & Dual, J. (2012). Multiple defect detection by applying the time reversal principle on dispersive waves in beams. *E-journal of nondestructive testing*, *17*(7), 1–9. http://www.ndt.net/?id=12790

[2] Zhang, J., Drinkwater, B. W., Wilcox, P. D., & Hunter, A. J. (2010). Defect detection using ultrasonic arrays: The multi-mode total focusing method. *NDT & e international*, *43*(2), 123–133. https://doi.org/10.1016/j.ndteint.2009.10.001

[3] Ludwig, R., & Lord, W. (1986). Developments in the finite element modeling of ultrasonic NDT phenomena. *Conference proceedings and presentations*, 73–81. https://doi.org/10.1007/978-1-4615-7763-8_7

[4] Baskaran, G., Rao, C. L., & Balasubramaniam, K. (2007). Simulation of the TOFD technique using the finite element method. *Insight-non-destructive testing and condition monitoring*, *49*(11), 641–646. https://doi.org/10.1784/insi.2007.49.11.641

[5] Honarvar, F., & Khorasani, S. (2010). Simulation of time of flight diffraction (ToFD) technique by finite element method. *E-journal of nondestructive testing (EJNDT)*, *15*(5), 1–8. https://www.ndt.net/article/SimNDT2010/papers/16_Honarvar_Rev1.pdf

[6] Hosseini, S. H., & Honarvar, F. (2023). A numerical model for ultrasonic time-of-flight diffraction (TOFD) testing of austenitic welds. *Russian journal of nondestructive testing*, *59*(2), 182–203. https://doi.org/10.1134/S106183092360003X

[7] Dai, X., Lu, C., & Zheng, M. F. (2014). FEM analyses of the tofd technique in unequal thickness component. *Recent research on mechanical engineering, mechatronics and automation* (Vol. 574, pp. 427–431). Trans Tech Publications Ltd. https://doi.org/10.4028/www.scientific.net/AMM.574.427

[8] Silk, M. G. (1976). The determination of crack penetration using ultrasonic surface waves. *NDT international*, *9*(6), 290–297. https://doi.org/10.1016/0308-9126(76)90071-7

[9] Date, K., Shimada, H., & Ikenaga, N. (1982). Crack height measurement — an evaluation of the accuracy of ultrasonic timing methods. *NDT international*, *15*(6), 315–319. https://doi.org/10.1016/0308-9126(82)90068-2

[10] Hévin, G., Abraham, O., Pedersen, H. A., & Campillo, M. (1998). Characterization of surface cracks with Rayleigh waves: A numerical model. *NDT & e international*, *31*(4), 289–297. https://doi.org/10.1016/S0963-8695(98)80013-3

[11] Scala, C. M., & Bowles, S. J. (2000). Laser ultrasonics for surface-crack depth measurement using transmitted near-field Rayleigh waves. *AIP conference proceedings*, *509*(1), 327–334. https://doi.org/10.1063/1.1306068

[12] Verma, B., & Bélanger, P. (2024). Surface breaking crack sizing method using pulse-echo Rayleigh waves. *Ultrasonics*, *138*, 107232. https://doi.org/10.1016/j.ultras.2023.107232

[13] Liu, Z., Li, Z., Lyu, D., Zhang, Z., & Hu, H. (2025). Imaging method of surface defect using leaky Rayleigh wave with ultrasonic phased array. *Nondestructive testing and evaluation*, *40*(6), 2311–2328. https://doi.org/10.1080/10589759.2024.2377726

[14] Verma, B., & Bélanger, P. (2023). An alternative Rayleigh wave excitation method using an ultrasonic phased array. *Ultrasonics*, *135*, 107121. https://doi.org/10.1016/j.ultras.2023.107121

[15] Xiao, J., Hu, Y., Cao, S., & Cui, F. (2023). Characterization of surface-breaking cracks on tubular structures using ultrasonic phased array with rayleigh waves. *International journal of computational methods*, *20*(06), 2143005. https://doi.org/10.1142/S0219876221430052

[16] Vu, A., Madhuranthakam, Y., Poudel, A., & Chakrapani, S. K. (2023). Numerical study of rayleigh wave interaction with rolling contact fatigue type of defects. *Research in nondestructive evaluation*, *34*(1), 38–50. https://doi.org/10.1080/09349847.2023.2180560

[17] Kolkoori, F. D. S., Koch, S. D. R., & Falter, T. D. S. (2024). 3D hybrid modeling for the ultrasonic phased array inspection of porosity in heavy plates: Application simulation and experimental validation. *E-journal of nondestructive testing*, *1*(1), 1–10. https://doi.org/10.58286/28218

[18] Xu, Q., & Wang, H. (2022). Sound field modeling method and key imaging technology of an ultrasonic phased array: A review. *Applied sciences*, *12*(16), 7962. https://doi.org/10.3390/app12167962

[19] Torbali, M. E., Zolotas, A., Avdelidis, N. P., Alhammad, M., Ibarra-Castanedo, C., & Maldague, X. P. (2024). A complementary fusion-based multimodal non-destructive testing and evaluation using phased-array ultrasonic and pulsed thermography on a composite structure. *Materials*, *17*(14), 3435. https://doi.org/10.3390/ma17143435

[20] Xiao, J., & Cui, F. (2023). Machine learning enhanced characterization of surface defects using ultrasonic Rayleigh waves. *NDT & e international*, *140*, 102969. https://doi.org/10.1016/j.ndteint.2023.102969

[21] Sanchez Duo, I., Lanzagorta, J. L., Aizpurua Maestre, I., & Galdos, L. (2024). Enhancing time-of-flight diffraction (TOFD) inspection through an innovative curved-sole probe design. *Sensors*, *24*(19), 6360. https://doi.org/10.3390/s24196360

[22] Cheng, Q., He, J., Yang, S., Gu, X., Huang, H., & Luo, Y. (2023). Propagation characteristics of ultrasonic waves generated by phased array laser in coating/substrate structure. *International journal of thermophysics*, *44*(8), 116. https://doi.org/10.1007/s10765-023-03225-y

[23] Bachhav, K. J., Gantala, T., & Balasubramaniam, K. (2024). guided wave phased array ultrasonic imaging for thin plate inspection. *E-journal of nondestructive testing*, *29*(7), 1–6. https://doi.org/10.58286/29801

[24] Connolly, G. D. (2009). *Modelling of the propagation of ultrasound through austenitic steel welds* [**Thesis**]. https://www.imperial.ac.uk/media/imperial-college/research-centres-and-groups/non-destructive-evaluation/GDConnolly-thesis.pdf